2D inversion for plane wave EM methods using an adaptive unstructured grid finite element approach: formulation, calculation of sensitivities and first results

Baranwal[1] V.C., Franke[1] A., Börner[1] R.-U., Spitzer[1] K., Sharma[2] S.P.

1. Institute of Geophysics, Freiberg University of Mining and Technology, Freiberg, Germany
2. Dept. of Geology and Geophysics, Indian Institute of Technology Kharagpur, India

Abstract

We present a 2D damped least-squares inversion approach for plane wave methods using an adaptive unstructured grid finite element forward operator. The development of an efficient inversion scheme to interpret two-dimensional (2D) magnetotelluric (MT) and very low frequency (VLF) data sets needs the elaborate calculation of the sensitivity matrix that contains the partial derivatives of the data with respect to the inversion model parameters. The perturbation method that determines the sensitivity matrix row-wise requires $(m+1)n_f$ forward computations, where m is the number of model parameters and n_f the number of frequencies. The same numerical effort arises for another procedure called the sensitivity equation method that provides one linear system of equations for each row of the Jacobian matrix. However, it can be reduced to $(n+1)n_f$ forward calculations where n is the number of observation points. This method uses a modified equation system obtained from the derivative of the finite element equations with respect to the model parameters.

For the forward calculations we use an adaptive unstructured grid finite element algorithm that allows for efficient discretisation of arbitrary 2D model geometries. However, the inversion model is parameterised on a coarser grid, for which the sensitivities are determined. Due to the small number of degrees of freedom the numerical effort is relatively low. So far, the procedure is implemented for inversion of E-polarisation data sets which is particularly relevant to the VLF method, however, the approach for inversion of H-polarisation will follow analogously without large effort. We show that the inversion process converges and gives reasonable results for simple cases. Concluding, we obtain a two-grid technique which has proved to be numerically efficient.

Introduction

Data inversion is a mathematical approach to fit the physical response computed for a parameter model to the observed data. In the last decades, inversion approaches have been developed by various researchers for 1D, 2D and 3D MT data (Jupp & Vozoff, 1975; deGroot-Hedlin & Constable, 1990; Smith & Booker, 1991; Mackie & Madden, 1993; Siripunvaraporn & Egbert, 2000; Rodi & Mackie, 2001). 1D MT data inversions are too simple to cope with a complex earth. However, 3D MT data inversions are very time consuming and large computer memory is required to solve the problem. In cases, where the assumption of 2D subsurface structures is valid, 2D inversion approaches serve as a rapid and numerically inexpensive alternative to obtain significant models.

A good review of inversion schemes is presented by Günther (2004). Among other methods, the Gauss-Newton or least-squares method is well known to minimise an appropriate objective function. Levenberg (1944) introduced the use of a Lagrange parameter to the Gauss-Newton approach. The method is described in detail by Marquardt (1963) and since then has been known as the Marquardt-Levenberg Method. Some researchers have referred it as damped least-squares method (Oristaglio & Worthington, 1980; Raiche et al., 1985) or ridge regression method (Inman, 1975). The damped least-squares method serves as a hybrid between the steepest descent and the Gauss-Newton methods (Lines & Treitel, 1984).

All the inversion schemes based on the minimisation of an objective function require the computation of the Jacobian or sensitivity matrix which consists of the partial derivatives of the observed data with respect to the

inversion model parameters. The perturbation or brute-force, the sensitivity-equation and the adjoint-equation method can be applied for the calculation of the sensitivity matrix (Rodi, 1976; McGillivray & Oldenburg, 1990; McGillivray et al., 1994; Farquharson & Oldenburg, 1996).

We have focussed on a discrete inversion approach of 2D MT data using the modified sensitivity-equation method (Rodi, 1976) for calculating the Jacobian. The region of interest is parameterised in rectangular blocks with piecewise constant electrical conductivities. The size of the rectangular blocks remains unchanged during the inversion process. Only the conductivities of the rectangular blocks vary to get an appropriate fitting of the computed to the observed data. We calculate the forward response on the basis of an adaptive unstructured grid finite element approach. Hence, we apply different parameterisation and discretisation schemes for forward modelling and inversion. All the codes are developed using MATLAB®.

Forward Modelling

The propagation of electromagnetic fields is governed by Maxwell's equations. In the case of plane-wave, diffusive, time-harmonic electromagnetic fields in 2D conductivity structures they can be combined to yield two decoupled equations of induction

$$\frac{\partial^2 E_y}{\partial^2 x^2} + \frac{\partial^2 E_y}{\partial^2 z^2} - i\omega\mu\sigma E_y = 0, \tag{1}$$

$$\frac{\partial}{\partial x}\left(\frac{1}{\sigma}\frac{\partial H_y}{\partial x}\right) + \frac{\partial}{\partial z}\left(\frac{1}{\sigma}\frac{\partial H_y}{\partial z}\right) - i\omega\mu H_y = 0 \tag{2}$$

for E-polarisation and H-polarisation, respectively, in a right-handed Cartesian coordinate system with the positive z-axis pointing upwards. E_y is the electric field and H_y is the magnetic field. y denotes the strike direction. ω, μ, i, and σ are angular frequency, magnetic permeability, imaginary unit, and electrical conductivity, respectively. To solve for the unknown fields, inhomogeneous Dirichlet boundary conditions are applied that assign the field values for a horizontally layered half-space at the boundaries.

The forward computations are carried out by an adaptive unstructured triangular grid finite element (FE) algorithm (Franke et al., 2004). An adaptive mesh refinement is applied to get sufficiently fine meshes at conductivity contrasts. Additionally, the grid gets coarser towards greater depths and towards the boundaries due to a geometrical criterion that limits the adaptive refinement to the central region of the model. Adaptive mesh refinement redistributes the nodes of a uniform mesh in regions where a large number of nodes are required to guarantee a proper sampling of steep spatial field variations.

The FE discretisation leads to a system of equations that can be expressed in matrix-vector form as

$$\left(\tilde{K} + \tilde{M}\right)\vec{u} = 0, \tag{3}$$

where $\vec{u}$ is the column vector of the electric field values E_y and the magnetic field values H_y at each node in E-polarisation and H-polarisation, respectively. $\tilde{K}$ and $\tilde{M}$ are referred to as stiffness and mass matrix.

The remaining field components H_x, H_z for E-polarisation and E_x, E_z for H-polarisation can be determined at each grid node by

$$H_x = \frac{1}{i\omega\mu}\frac{\partial E_y}{\partial z} \quad , \quad H_z = -\frac{1}{i\omega\mu}\frac{\partial E_y}{\partial x},$$
$$E_x = -\frac{1}{\sigma}\frac{\partial H_y}{\partial z} \quad , \quad E_z = \frac{1}{\sigma}\frac{\partial H_y}{\partial x}. \tag{4}$$

The apparent resistivity ρ_a and the phase ϕ can be computed

for E-polarisation as

$$\rho_a = \frac{1}{\omega\mu}\left|\frac{E_y}{H_x}\right|^2 \quad \text{and} \quad \phi = tan^{-1}\left(\frac{\mathrm{Im}(E_y/H_x)}{\mathrm{Re}(E_y/H_x)}\right) \tag{5}$$

and for H-polarisation as

$$\rho_a = \frac{1}{\omega\mu}\left|\frac{E_x}{H_y}\right|^2 \quad \text{and} \quad \phi = tan^{-1}\left(\frac{\mathrm{Im}(E_x/H_y)}{\mathrm{Re}(E_x/H_y)}\right). \tag{6}$$

Inversion procedure

We apply the damped least-squares method for minimisation of the objective function ψ given by

$$\psi = \left(\Delta\vec{d} - S\Delta\vec{p}\right)^T\left(\Delta\vec{d} - S\Delta\vec{p}\right) + \lambda\left(\Delta\vec{p}^T\Delta\vec{p} - p_0^2\right), \tag{7}$$

where $\Delta\vec{d} = (\vec{d}^{obs} - \vec{d}^{comp})$ denotes the discrepancy vector. $\vec{d}^{obs}$ represents the observed data and $\vec{d}^{comp}$ is the computed data for the assumed model. S and $\Delta\vec{p}$ denote the sensitivity matrix and the model parameter update, respectively. The logarithmised conductivities are considered as model parameters. The Lagrange parameter λ is introduced to constrain the energy of the model parameter update to a finite quantity p_0^2. To get the minimum of the objective function ψ, its partial derivatives $\partial\psi/\partial\Delta p_j$ are required to be zero corresponding to all j. Therefore, deriving eq. (7) partially with respect to Δp_j and setting it to zero gives

$$S^T S\Delta\vec{p} + \lambda\Delta\vec{p} = S^T\Delta\vec{d}, \tag{8}$$

which can be rearranged to solve for the model parameter updates as

$$\Delta\vec{p} = \left(S^T S + \lambda I\right)^{-1} S^T\Delta\vec{d}. \tag{9}$$

As appears in eq. (9), the Lagrange parameter λ prevents $S^T S$ from being singular. It also damps large oscillating changes in the model parameters which may lead to unstable solutions during inversion process.

Logarithmic values of apparent resistivity and the phase in radian are used as data which assures both to have similar numerical values. The use of the logarithm of conductivities as model parameter prevents them to become negative during inversion. However, it may become unrealistically large when the solution starts to diverge.

The model parameters are updated by

$$p_j^{new} = p_j^{old} e^{\Delta p_j}. \tag{10}$$

Equation (9) has been solved iteratively applying a direct solver and model parameters are updated by eq. (10) after each iteration. We have applied three criteria to stop the iteration: (1) by defining the maximum number of iterations, (2) if the change in the error measure from one iteration to the next is less than 0.01%, and (3) when $\chi^2 \approx 1$.

The root mean square (RMS) error and χ^2-value can be calculated by

$$RMS = \sqrt{\sum_{i=1}^{n}\frac{\left(d_i^{obs} - d_i^{comp}\right)^2}{n}} \quad , \quad \chi^2 = \frac{1}{n}\sum_{i=1}^{n}\frac{\left(d_i^{obs} - d_i^{comp}\right)^2}{\epsilon_i^2}, \tag{11}$$

where ϵ_i is the standard deviation of the error in the data. The χ^2-criteria is well accepted due to the fact that noise in MT data is assumed as normally distributed. If the amount of noise is known in the observed data then the χ^2-criteria stops the inversion before the noise is fitted (Whittall & Oldenburg, 1992).

There remains the open problem to select an appropriate value of the Lagrange parameter λ. The L-curve and generalised cross validation (GCV) criterion can be used for the selection of proper starting λ-value. We have observed that the maximum singular value of $S^T S$ proves to be sufficient as the starting value for λ.

To get fast convergence, λ is decreased by a factor of less than one (e.g. 0.5) in each iteration. Whenever the solution starts to diverge i.e. the RMS error in the current iteration is more than the RMS error in the previous iteration, λ is increased again to make the solution stable. The introduction of λ in this fashion allows resolving of prominent model parameters (having largest singular values) first and model parameters with smaller singular values later.

We need to investigate the behaviour of the convergence to find an appropriate factor to decrease λ in each iteration. If the χ^2-value converges very fast or the solution starts to diverge before reaching the χ^2-criterion then a larger factor is required to decrease λ so that we get $\chi^2 \approx 1$ in the last iteration before stopping the inversion process.

Sensitivity calculation

Here, we show how to determine the sensitivities for E-polarisation. In principle, the sensitivities may be computed by three methods: (1) the brute-force method, (2) the sensitivity-equation method, and (3) the adjoint-equation method.

For m model parameters, n observation locations, and n_f frequencies, the brute-force and the sensitivity-equation methods require $(m+1)n_f$ forward computations whereas the adjoint-equation method requires $(n+1)n_f$ forward computations.

Rodi (1976) has presented the efficient use of the sensitivity-equation method to compute sensitivities in a modified form depending on whether there are more observation points than model parameters or vice versa. The modified sensitivity-equation method requires $(n+1)n_f$ forward computations. Therefore, one of these sensitivity-equation methods can be used to calculate sensitivities depending on the actual number of parameters and observation sites. We have used the modified sensitivity-equation method for the calculation of the sensitivities. The same approach is used by Rodi and Mackie (2001) and Siripunvaraporn and Egbert (2000) for MT inversion and by Zhang et al. (1995) for DC resistivity inversion. Expressions for sensitivities of logarithmised apparent resistivity $S_{ij}^{ln\rho_a}$ and phase S_{ij}^{ϕ} for the i^{th} observation site and j^{th} model parameter can be computed by evaluating a complex quantity S_{ij} as

$$S_{ij}^{ln\rho_a} = 2\text{Re}(S_{ij}) \quad , \quad S_{ij}^{\phi} = \text{Im}(S_{ij}), \tag{12}$$

where S_{ij} will be expressed according to Farquharson and Oldenburg (1996) as

$$S_{ij} = \frac{1}{E_y}\frac{\partial E_y}{\partial \sigma_j} - \frac{1}{H_x}\frac{\partial H_x}{\partial \sigma_j}. \tag{13}$$

The electric field E_y and the magnetic field H_x at the i^{th} observation site can be computed from $\vec{u}$ by forming two column vectors $\vec{a_i}$ and $\vec{b_i}$ as

$$E_y = \vec{a_i}^T \vec{u} \quad , \quad H_x = \vec{b_i}^T \vec{u}. \tag{14}$$

$\vec{a_i}$ is formed by simply keeping 1 at the position of the i^{th} datum and zeros at all other nodes. $\vec{b_i}$ is designed to perform also a numerical differentiation over $\vec{u}$ according to eq. (4) and gives H_x value at the i^{th} observation site when used according to eq. (14). If the observation site is not located excatly at the discretised grid node then it is interpolated by two nearby grid nodes.

Now inserting the values of E_y and H_x into eq. (13) and using eq. (3) gives

$$S_{ij} = \left(\frac{1}{\vec{a_i}^T \vec{u}}\vec{a_i} - \frac{1}{\vec{b_i}^T \vec{u}}\vec{b_i}\right)^T \left(\tilde{K} + \tilde{M}\right)^{-1} \left(-\frac{\partial \tilde{M}}{\partial \sigma_j}\right) \vec{u}, \tag{15}$$

Since $(\tilde{K}+\tilde{M})$ is a symmetric matrix, a vector v_i can be introduced so that $\vec{v_i}^T = (\frac{1}{\vec{a_i}^T\vec{u}}\vec{a_i} - \frac{1}{\vec{b_i}^T\vec{u}}\vec{b_i})^T(\tilde{K}+\tilde{M})^{-1}$. $\vec{v_i}^T$ is evaluated by solving a modified forward problem as

$$\left(\tilde{K}+\tilde{M}\right)\vec{v_i} = \left(\frac{1}{\vec{a_i}^T\vec{u}}\vec{a_i} - \frac{1}{\vec{b_i}^T\vec{u}}\vec{b_i}\right). \tag{16}$$

$\vec{u}$ is solved from eq. (3) and the value of $-\partial\tilde{M}/\partial\sigma_j$ can be calculated easily without much effort, hence, all the parameters are known to solve eq. (15). Therefore, a total of $n+1$ forward computations are required to be solved for each frequency to calculate the sensitivities. One forward computaion is required to solve eq. (3) for $\vec{u}$ and n forward computations are required to solve eq. (16) corresponding to n observation sites. The values of S_{ij} are used to compute the desired sensitivities $S_{ij}^{ln\rho_a}$ and S_{ij}^{ϕ} according to eq. (12).

Results and discussion

We present inversion results of an E-polarisation data set. The synthetic data are calculated for an assumed model and Gaussian noise is added to the synthetic data.

Synthetic Model

We consider a simple model (Fig. 1 left) for testing the performance of our inversion code. The model consists of an anomalous region having a conductivity of $0.1\,\mathrm{S/m}$ and a size of $300\,\mathrm{m} \times 150\,\mathrm{m}$ within a $0.01\,\mathrm{S/m}$ half-space. The forward response is calculated at 9 different locations (arrows in Fig. 1 right)) ranging from $-1000\,\mathrm{m}$ to $1000\,\mathrm{m}$ with $250\,\mathrm{m}$ spacing for frequencies $1000\,\mathrm{Hz}$, $500\,\mathrm{Hz}$ and $100\,\mathrm{Hz}$. $5\,\%$ Gaussian noise is added to the apparent resistivity and an equivalent of $1.5\,^\circ$ is added to the phase data.

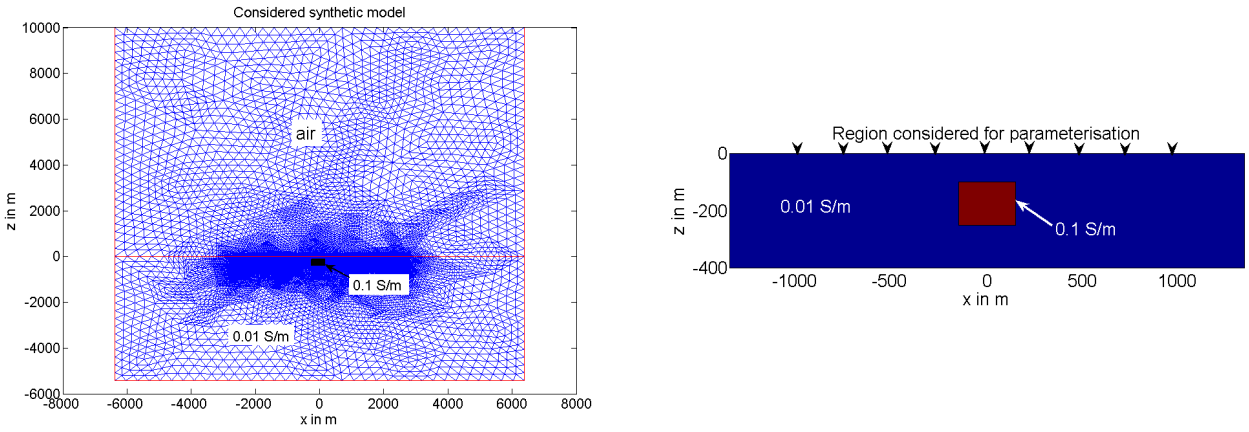

Figure 1: Synthetic model of a buried rectangular $0.1\,\mathrm{S/m}$ body ($300\,\mathrm{m} \times 150\,\mathrm{m}$) within a half-space of $0.01\,\mathrm{S/m}$ for generating the synthetic data (left). The region considered for parameterisation to perform the inversion (right). Observation sites are marked by arrows.

Inversion results

We select a region as shown in Fig. 1 (right) for parameterisation to perform the inversion. The region is parameterised in rectangular blocks. The size of the blocks is fixed in the x-direction and increases by a factor of 1.5 in the z-direction. Two differently parameterised models with half-spaces of $0.01\,\mathrm{S/m}$ conductivity are assumed as starting models to test the inversion approach for different parameterisations. The first starting model for the

inversion is parameterised in such a manner that the anomalous region accomodates exactly in the parameterised region. Basic block size is considered as $100\,\mathrm{m} \times 100\,\mathrm{m}$ for parameterisation. Minimisation stops after 5 iterations when $\chi^2 \approx 1$ (Fig. 2). The λ-value is decreased by a factor of 0.6 in each iteration. Fig. 3 depicts that inversion of the synthetic data is able to resolve the anomalous region and the conductivities of this region are also close to their true values. The fitting between observed and computed data is good as shown in Fig. 4.

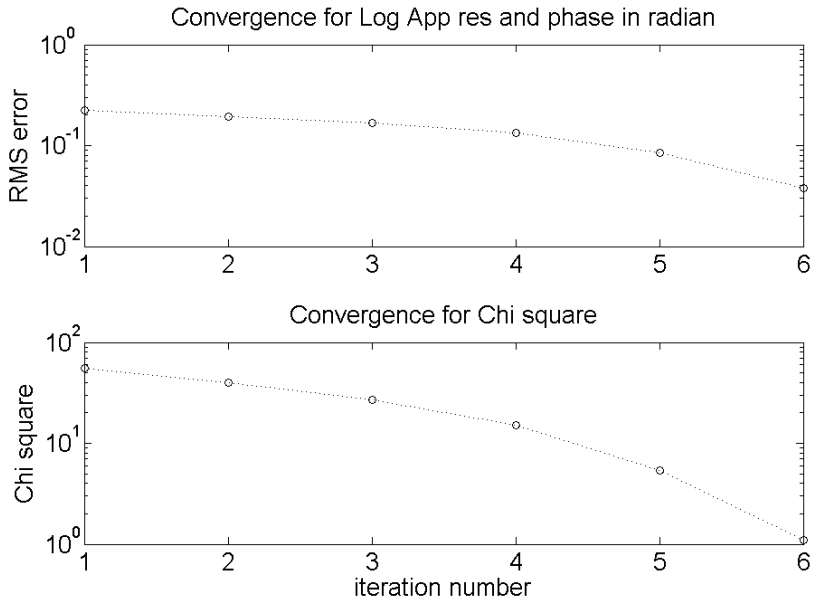

Figure 2: Convergence of RMS error and χ^2-value during the iteration. Minimisation is stopped when $\chi^2 \approx 1$.

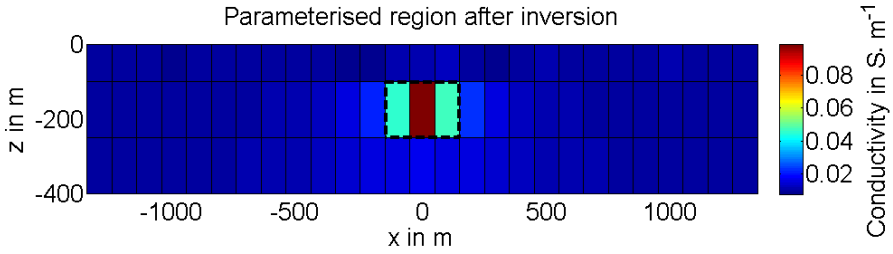

Figure 3: Model obtained from inversion using a $0.01\,\mathrm{S/m}$ half-space as starting model. Parameterisation accomodates the anomalous region exactly (covered by dashed lines).

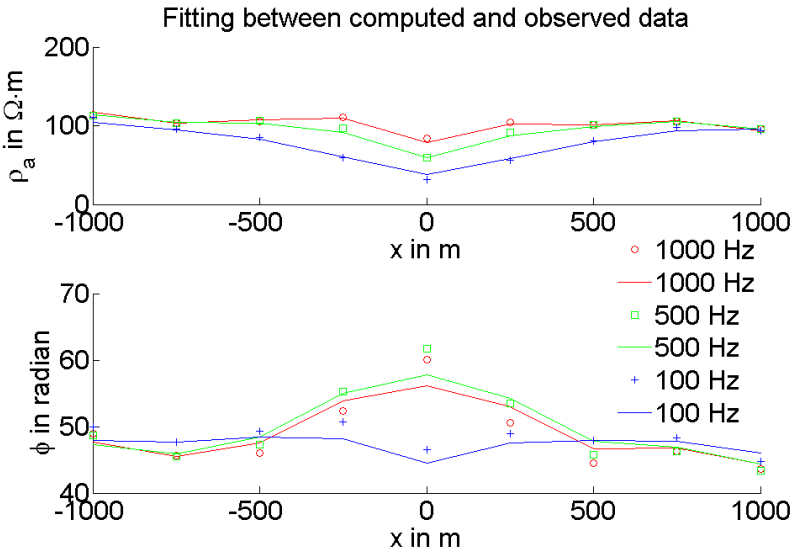

Figure 4: Fitting between observed and computed apparent resistivity and phase data. Symbols represent observed data and solid lines represent computed data.

The second starting model for the inversion uses the same half-space. However, the parameterisation is finer compared to the previous one and does not coincide with the outline of the perturbing body. Basic block size is considered as $50\,\mathrm{m} \times 20\,\mathrm{m}$ for parameterisation. Minimisation stops after 5 iterations (Fig. 5). The λ-value is decreased by a factor of 0.5 in each iteration. The inverted model shows that the inversion result is close to the assumed model but some of the blocks in the upper corners of the anomalous region of the inverted model are not well resolved (Fig. 6). This may be due to the disagreement of the parameterisations and the higher degree of ill-posedness due to the larger number of parameters. However, the fitting is good for all frequencies (Fig. 7).

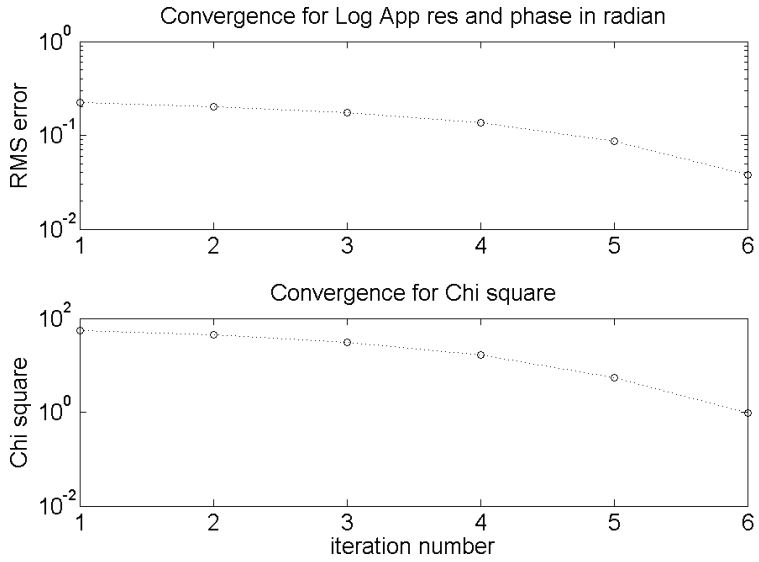

Figure 5: Convergence of RMS error and χ^2-value during the iteration for the second model. Minimisation is stopped when $\chi^2 \approx 1$.

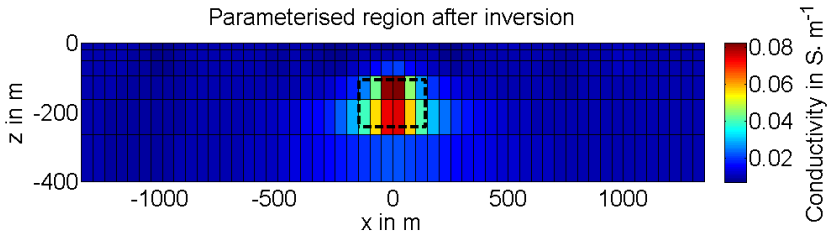

Figure 6: Model obtained after inversion. The starting model is a half-space of conductivity $0.01\,\mathrm{S/m}$. Parameterisation is finer than the one used for the previous starting model and not able to accomodate the anomalous region exactly (covered by dashed lines).

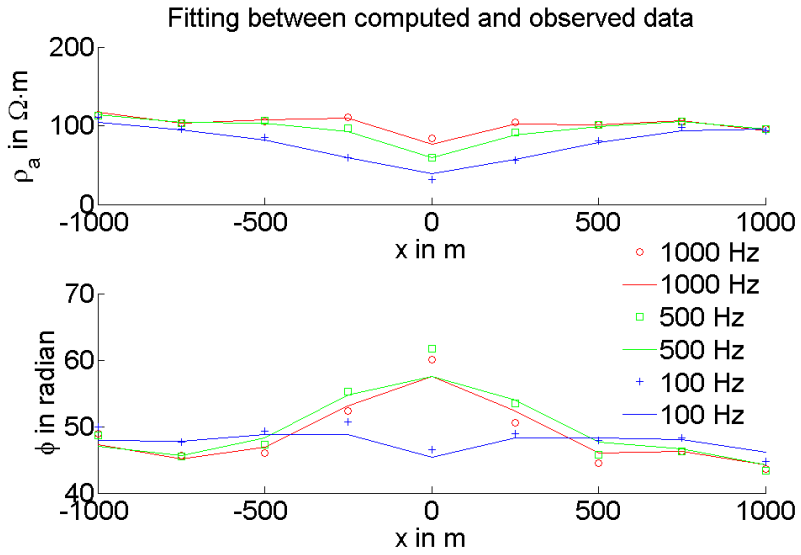

Figure 7: Fitting between observed and computed apparent resistivity and phase data for the second model. Symbols represent observed data and solid lines represent computed data.

Conclusion

This is the first step in the development of a new 2D inversion approach. We have shown that the algorithm works in principle. The elements of the sensitivity matrix are calculated by the modified sensitivity equation method which is efficient when the number of observation points is smaller than the number of model parameters.

Different discretisation and parameterisation schemes are used in forward modelling and inversion. The forward

simulation is done applying an adaptive unstructured triangular grid finite element algorithm that enables us to model nearly any 2D conductivity structure including surface topography. However, the inversion is carried out by parameterising the region of interest in rectangular blocks. This has to be considered as a first test of operational reliability. We will enhance the parameterisation to include topography in the inverse process as well and to exploit the full power of the forward operator. Mapping between forward modelling grid and parameterisation grid of the inverse model will thus become an important issue of our future research.

References

deGroot-Hedlin, C., & Constable, S. (1990). Occam inversion to generate smooth, two-dimensional models for magnetotelluric data. *Geophysics*, *55*, 1613-1624.

Farquharson, C. G., & Oldenburg, D. W. (1996). Approximate sensitivities for the electromagnetic inverse problem. *Geophys. J. Int.*, *126*, 235-252.

Franke, A., Börner, R.-U., & Spitzer, K. (2004). 2d finite element modelling of plane-wave diffusive time-harmonic electromagnetic fields using adaptive unstructured grids: Extended abstract. *17th Workshop on Electromagnetic Induction in the Earth, Hyderabad, India. www-document. http://www.emindia2004.org.*, *S.2-O.01*, 1-6.

Günther, T. (2004). *Inversion methods and resolution analysis for the 2d/3d reconstruction of resistivity structures from dc measurements*. Unpublished doctoral dissertation, TU Begakademie Freiberg, Freiberg, Germany.

Inman, J. R. (1975). Resistivity inversion with ridge regression. *Geophysics*, *40*, 798-817.

Jupp, D. L. B., & Vozoff, K. (1975). Stable iterative methods for the inversion of geophysical data. *Geophys. J. R. astr. Soc.*, *42*, 957-976.

Levenberg, K. (1944). A method for the solution of certain nonlinear problems in least squares. *Quarter. Appl. Mathemat.*, *2*, 164-168.

Lines, L. R., & Treitel, S. (1984). Tutorial: A review of least-squares inversion and its application to geophysical problems. *Geophys. Prospect.*, *32*, 159-186.

Mackie, R. L., & Madden, T. R. (1993). Three-dimensional magnetotelluric inversion using conjugate gradients. *Geophys. J. Int.*, *115*, 215-229.

Marquardt, D. W. (1963). An algorithm for least squares estimation of non-linear parameters. *J. Soc. Indus. Appl. Mathemat.*, *11*, 431-441.

McGillivray, P. R., & Oldenburg, D. W. (1990). Methods for calculating frechet derivatives and sensitivities for the non-linear inverse problem: a comparative study. *Geophys. Prospect.*, *38*, 499-524.

McGillivray, P. R., Oldenburg, D. W., Ellis, R. G., & Habashy, T. M. (1994). Calculation of sensitivities for the frequency-domain electromagnetic problem. *Geophys. J. Int.*, *116*, 1-4.

Oristaglio, M. L., & Worthington, M. H. (1980). Inversion of surface and borehole electromagnetic data for two-dimensional electromagnetic conductivity models. *Geophys. Prospect.*, *28*, 633-657.

Raiche, A. P., Jupp, D. L. B., Rutter, H., & Vozoff, K. (1985). The joint use of coincident loop transient electromagnetic and schlumberger sounding to resolve layered structures. *Geophysics*, *50*, 1618-1627.

Rodi, W. L. (1976). A technique for improving the accuracy of finite element solutions for magnetotelluric data. *Geophys. J. R. astr. Soc.*, *44*, 483-506.

Rodi, W. L., & Mackie, R. L. (2001). Nonlinear conjugate gradient algorithm for 2-d magnetotelluric inversion. *Geophysics*, *66*, 174-187.

Siripunvaraporn, W., & Egbert, G. (2000). An efficient data-subsurface inversion method for 2-d magnetotelluric data. *Geophysics*, *65*, 791-803.

Smith, J. T., & Booker, J. R. (1991). Rapid inversion of two-and three-dimensional magnetotelluric data. *J. geophys. Res.*, *96*, 3905-3922.

Whittall, K. P., & Oldenburg, D. W. (1992). *Inversion of magnetotelluric data for a one-dimensional conductivity: Geophysical monograph series*. Soc. Expl. Geophys., Tulsa, OK.

Zhang, J., Mackie, R. L., & Madden, T. R. (1995). 3-d resistivity forward modelling and inversion using conjugate gradients. *Geophysics*, *60*, 1313-1325.